reactions are purely quantum in nature. There is, for example, little classical about the time-dependent picture where the ultimate outcome of the deexcitation, i.e., product H + HD or H_2 + D, depends entirely upon the phase and amplitude characteristics of the wavefunction. Indeed, as repeatedly emphasized above, if, e.g., collisional effects are sufficiently strong so as to wipe out the phases, then reaction control is lost. Hence reaction dynamics is intimately linked to the wavefunction phases which are controllable through coherent optical phase excitation.

These results must be viewed in light of the history of molecular reaction dynamics over the past two decades. Possibly the most useful result of the reaction dynamics research effort has been the recognition that the vast majority of qualitatively important phenomena in reaction dynamics are well described by classical mechanics.[10] Quantum and semiclassical mechanics were viewed as necessary only insofar as they correct quantitative failures of classical mechanics for unusual circumstances and/or for the dynamics of very light particles. Considering reaction dynamics in traditional chemistry to be essentially classical in character, therefore, appeared to be essentially correct for the vast majority of naturally occurring molecular processes. Coherence played no role. The approach that we have introduced above makes clear, however, that coherence phenomena have great potential for application. By calling attention to the extreme importance of coherence phenomena to controlled chemistry, we herald the introduction of a new focus in atomic and molecular science, i.e., introducing coherence in controlled environments to modify reactions, a kind of coherence chemistry.

(10) See, for example: Bernstein, R. B.; Levine, R. D. *Molecular Reaction Dynamics*; Oxford Univ. Press: New York, 1987.

Early work on control was supported by the Petroleum Research Fund, administered by the American Chemical Society. Subsequent work was supported by the U.S. Office of Naval Research under Contract No. N00014-87-J-1204 and the Minerva Foundation, Munich, West Germany.

Photoionization Mass Spectrometric Studies of Free Radicals

J. BERKOWITZ

Chemistry Division, Argonne National Laboratory, Argonne, Illinois 60439

Received May 23, 1989 (Revised Manuscript Received August 16, 1989)

Free radicals have been fascinating to chemists for decades, partly because of their important but ephemeral nature as intermediates in chemical reactions, e.g., combustion and atmospheric processes. For example, the reaction OH + CO → H + CO_2 is the dominant source of CO_2 in the oxidation of hydrocarbons and is important in the chemistry of the upper atmosphere and in the formation of chemical smog. This reaction is believed to proceed through a COOH intermediate, but until very recently, this species had not been detected in the gas phase. The depletion of ozone in the stratosphere is attributed to the reaction of the free radical ClO with O_3. The chemical vapor deposition method of producing solid-state devices based on Si or Ge employs a plasma containing free-radical hydrides of Si and Ge.

Some early studies demonstrating the existence of free radicals in the gas phase were performed by electron-impact mass spectrometry.[1] However, neither structural information nor precise thermochemical data were forthcoming. Lossing and collaborators[2] improved and developed this technique, particularly for the determination of ionization potentials of free radicals. With the advent of vacuum ultraviolet photoionization methods, it became clear that electron impact suffered two disadvantages relative to photon impact: (a) lower energy resolution, even with the use of electron monochromators, and (b) the fundamental nature of the electron-impact ionization process, which blurs details (such as autoionization). According to theory,[3] the energy dependence of photoionization at or just beyond threshold for a particular ionic state is a step function, while with electron impact the probability for ionization increases linearly from 0 at threshold. Since the energy derivative of a line of constant slope is constant, the energy derivative of an idealized electron-impact curve near threshold appears as a step in the corresponding photoionization curve. Hence, the onset in photoionization is more abrupt and can be determined more precisely.

Two complementary methods of vacuum ultraviolet (vacuum UV) photoionization have evolved: photoelectron spectroscopy (PES) and photoionization mass spectrometry (PIMS). Typically, PES employs a monochromatic light source incident upon a gaseous target, and an electron energy analyzer to measure the

Joseph Berkowitz received a B.Chem.Engr. degree from New York University and M.S. and Ph.D. degrees from Harvard University (Physical Chemistry). He was a postdoctoral associate at the University of Chicago before joining Argonne Natione National Laboratory, where he is a Senior Physicist. He has been a visiting professor at the University of Illinois (Urbana) and at Northwestern University. His research interests include photoionization mass spectrometry and photoelectron spectroscopy, molecular structure and energetics, autoionization phenomena, high-temperature chemistry, and gas-phase chemical reactions. He was a Guggenheim Fellow (1965-66) and an Alexander von Humboldt Senior U.S. Scientist Awardee (1988). He is the author of *Photoabsorption, Photoionization and Photoelectron Spectroscopy* (Academic Press, 1979) and coorganizer and coeditor of the NATO ASI entitled *Molecular Ions: Geometric and Electronic Structures* (Plenum, 1983).

(1) Eltenton, G. C. *J. Chem. Phys.* **1942**, *10*, 403; **1947**, *15*, 455.
(2) Lossing, F. P. *Ann. N.Y. Acad. Sci.* **1957**, *67*, 499. Lossing, F. P.; Maeda, K.; Semeluk, G. P. *Recent Dev. Mass Spectrosc. Proc. Int. Conf. Mass Spectrosc., 1969* **1970**, 791-6. Also many individual papers published between the early 1950s and 1980s. See also: Holmes, J. L.; Lossing, F. P.; Maccoll, A. *J. Am. Chem. Soc.* **1988**, *110*, 7339. Holmes, J. L.; Lossing, F. P. *Ibid.* **1988**, *110*, 7343.
(3) Wigner, E. P. *Phys. Rev.* **1948**, *73*, 1002.

0001-4842/89/0122-0413$01.50/0

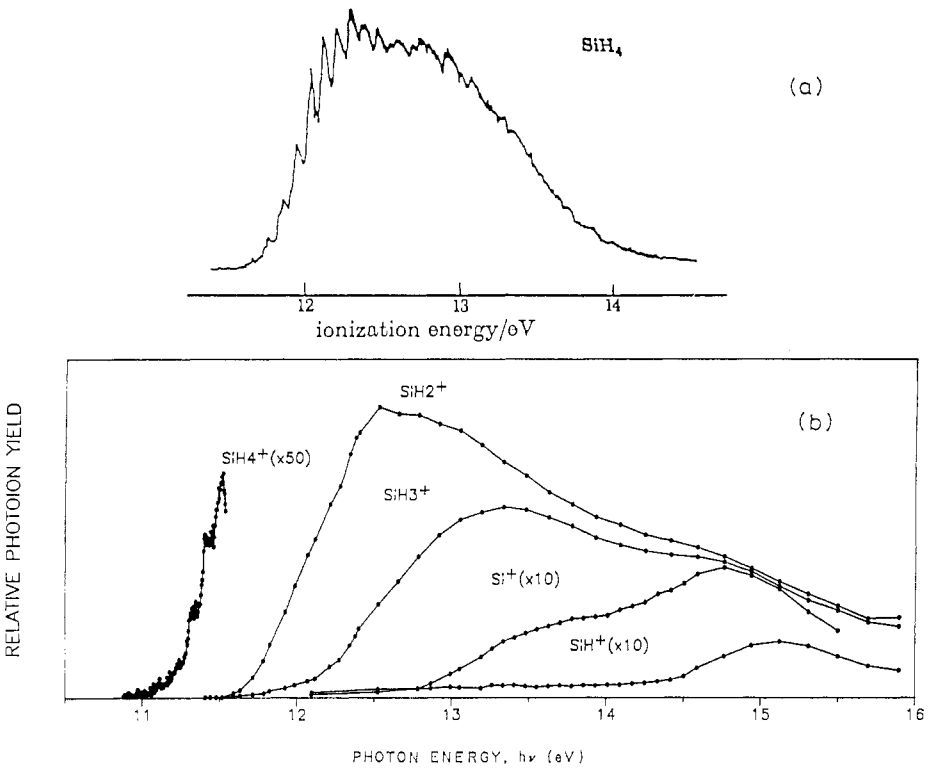

Figure 1. (a) He I PES of SiH_4 displaying an adiabatic threshold at 11.6 eV. Reprinted with permission from ref 6a. Copyright 1972 Royal Society (London). (b) PIMS of SiH_4 (from ref 7) displaying an adiabatic threshold at 11.00 eV.

kinetic energy spectrum of the ejected photoelectrons. This photoelectron spectrum[4] is often interpretable as single-electron ejection from the highest occupied molecular orbital and successively deeper ones. If vibrational structure is observed, it indicates that a change in geometrical structure has occurred between the neutral species and the cation, along the direction of the normal mode of the vibrational progression which has been excited. This information can be used quantitatively (utilizing the Franck–Condon approximation) to infer the structure of the cation, if the structure of the neutral molecule is known. This important property is extremely difficult, if not impossible, to extract from simple electron-impact studies. However, PES is usually performed without concomitant mass analysis. This can be particularly troublesome in the study of free radicals, since they are usually prepared from some precursor, and the photoelectron spectrum is a superposition of photoelectrons from all species present as target materials. In some cases of accidental overlap, subtractions must be performed which result in an uncertain "residue". Another problem is the typical dynamic range (from largest to smallest signal above background), which is perhaps 10^3 in PES. Within these constraints, a wide range of free radicals has been studied by PES, particularly by Dyke, Jonathan, and co-workers.[5]

By contrast, PIMS uses tunable vacuum UV radiation and measures the production of mass-analyzed photoions as a function of wavelength. Mass analysis usually eliminates the contribution from unwanted species (precursors, impurities) and also enhances the dynamic range. Consequently, the adiabatic ionization potential can be determined more precisely, but the onset of excited ionic states is not as clearly deduced as in PES and may even be obscured. From this brief description, it is apparent that a marriage of these techniques, such as photoion–photoelectron coincidence spectroscopy, is desirable. Such experiments are routinely performed on stable molecular species (where the superposition problem is not significant), but are more difficult to perform on free radicals, because the density of such transient species in the target region is substantially lower than that attainable with stable species.

Some Comparisons of PES and PIMS

The stable molecule SiH_4 provides a simple illustration of the greater dynamic range of PIMS. In the early 1970s, several investigators[6] published the photoelectron spectrum of SiH_4. A typical spectrum[6a] of the first band is shown in Figure 1a. The adiabatic ionization potential (IP) was reported to be 11.6 eV. By contrast, the PIMS of SiH_4 (Figure 1b)[7] reveals a weak parent ion, SiH_4^+, with a threshold of 11.00 eV. This is an enormous difference, when one considers the characteristic precision of these experiments (±0.01 eV). The new, lower IP has important structural consequences. Modern ab initio calculations[8] (performed after our experiment) reveal that SiH_4^+ undergoes extreme Jahn–Teller distortion; the ground state is better rep-

(4) Baker, A. D. *Acc. Chem. Res.* **1970**, *3*, 17.
(5) See, for example: (a) Dyke, J. M.; Jonathan, N.; Morris, A. *Int. Rev. Phys. Chem.* **1982**, *2*, 3–42. (b) Dyke, J. M. *J. Chem. Soc., Faraday Trans. 2* **1987**, *83*, 69–87. J. L. Beauchamp and co-workers have published, in *J. Am. Chem. Soc.*, a series of PES papers on hydrocarbon radicals formed by pyrolysis: **1978**, *100*, 3290; **1979**, *101*, 4067; **1984**, *106*, 3917; **1984**, *106*, 7336; **1986**, *108*, 2162; **1986**, *108*, 5441. See also: *J. Phys. Chem.* **1981**, *85*, 3456; **1985**, *89*, 5359.
(6) See, for example: (a) Potts, A. W.; Price, W. C. *Proc. R. Soc. (London)* **1972**, *A326*, 165. (b) Pullen, B. P.; Carlson, T. A.; Moddeman, W. E.; Schweitzer, G. K.; Bull, W. E.; Grimm, F. A. *J. Chem. Phys.* **1970**, *53*, 768.
(7) Berkowitz, J.; Greene, J. P.; Cho, H.; Ruscic, B. *J. Chem. Phys.* **1987**, *86*, 1235.
(8) (a) Pople, J. A.; Curtiss, L. A. *J. Phys. Chem.* **1987**, *91*, 155. (b) Frey, R. F.; Davidson, E. R. *J. Chem. Phys.* **1988**, *89*, 4227.

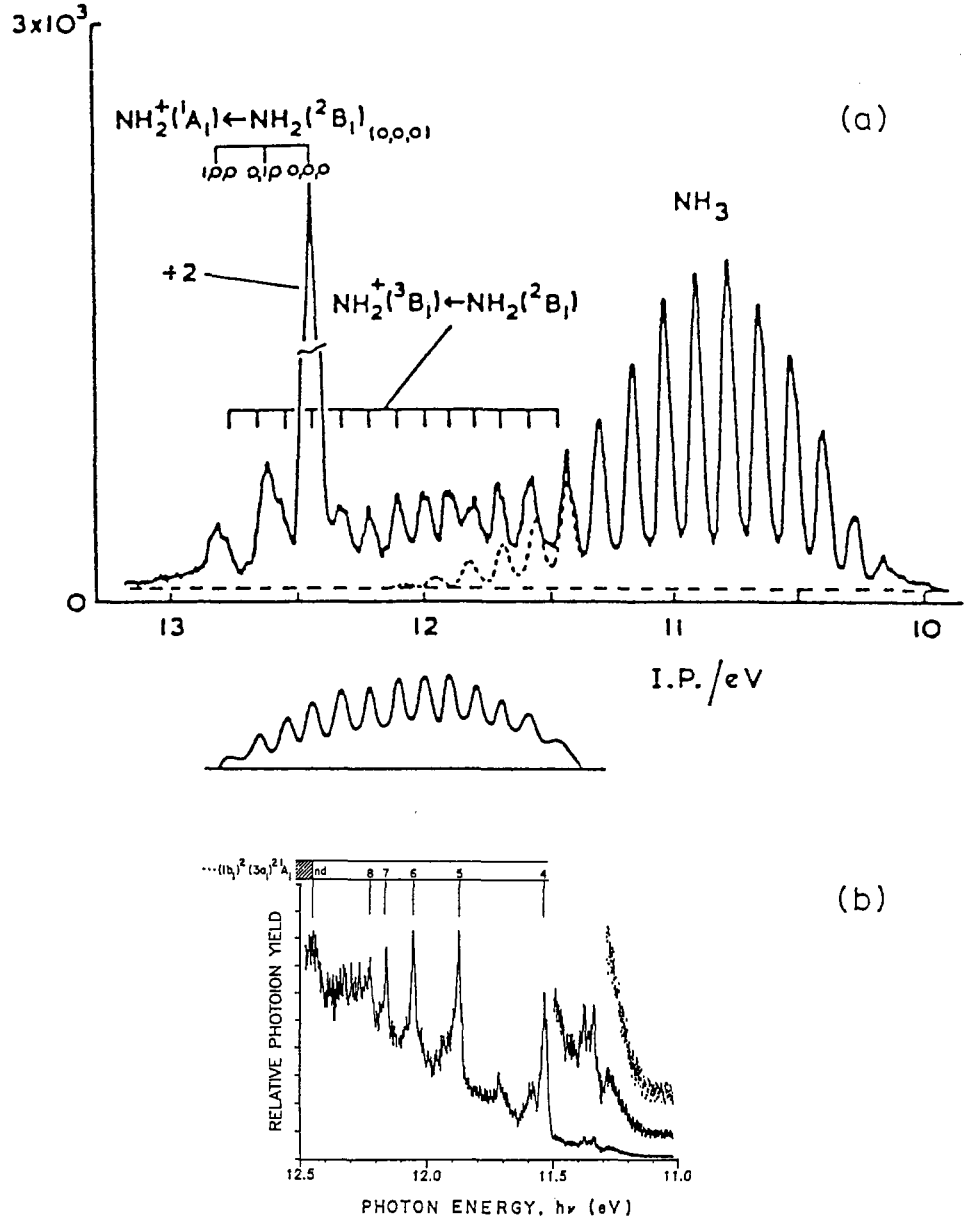

Figure 2. (a) He I PES of NH_2 displaying an adiabatic threshold for the $\tilde{X}^3B_1$ state at 11.46 eV and for the $^1A_1$ state at 12.45 eV. Reprinted with permission from ref 9. Copyright 1980 Taylor and Francis Ltd. (b) Photoion yield curve of NH_2 (from ref 10) displaying an adiabatic threshold for the $\tilde{X}^3B_1$ state at 11.14 ± 0.01 eV and convergence limit of the Rydberg autoionizing series to the $^1A_1$ state at 12.445 ± 0.002 eV.

resented as $SiH_2^+ \cdot H_2$. Hence, there is a very small overlap of the vibrational wave functions for tetrahedral SiH_4 and $SiH_2^+ \cdot H_2$ (very weak Franck–Condon factors). Detecting these weak onsets requires an apparatus with high sensitivity and low background.

The free radical NH_2 provides an example of the superposition problem. Figure 2a is a photoelectron spectrum of NH_2, with overlapping by a band from the precursor NH_3 molecule. From the subtracted spectrum (also shown), an adiabatic ionization potential of 11.46 eV was reported.[9] Figure 2b is a portion of the PIMS[10] of NH_2. The adiabatic ionization potential obtained is 11.14 eV, lower by 3 vibrational quanta and influencing derived bond energies by 7.4 kcal/mol.

The PH_2 species illustrates the difficulties encountered by both techniques. Figure 3a is a photoelectron spectrum[5a] obtained from the products of the F + PH_3 reaction. Several species are identified on this figure. We focus our attention on the second band of PH_2 (~11.1–11.6 eV). Clearly, it is difficult to extract the adiabatic onset of this band and, hence, the first excited state of PH_2^+. Figure 3b is a photoionization mass spectrum[11] of PH_2, produced by the H + PH_3 reaction. Although this spectrum is free of impurities, and its first adiabatic ionization potential is readily obtained (and agrees with PES), the onset of the excited state of PH_2^+ is obscured by structural features attributable to autoionization. Figure 3a illustrates another possible advantage of PIMS. In the generation of free radicals, consecutive reactions may occur, producing a variety of species. These must be judiciously assigned by PES, but are readily identified by PIMS. For example, the H + PH_3 reaction produces PH_2, PH, and P, each of which can be separately studied by PIMS. In the F +

(9) Dunlavey, S. J.; Dyke, J. M.; Jonathan, N.; Morris, A. *Mol. Phys.* **1980**, *39*, 1121.
(10) Gibson, S. T.; Greene, J. P.; Berkowitz, J. *J. Chem. Phys.* **1985**, *83*, 4319.
(11) Berkowitz, J.; Cho, H. *J. Chem. Phys.* **1989**, *90*, 1.

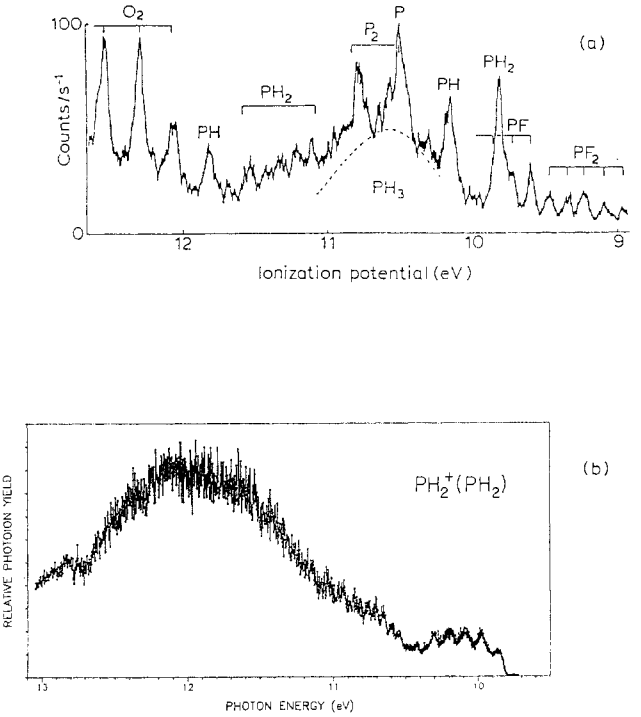

Figure 3. (a) He I PES of products from the F + PH_3 reaction. Reprinted with permission from ref 5a. Copyright 1980 Taylor and Francis Ltd. (b) Photoion yield curve of PH_2, from the H + PH_3 reaction (from ref 11).

SiH_4 reaction, only SiH_3 was observed by PES,[12] whereas SiH_3, SiH_2 (two states), and SiH could be measured by PIMS.[7]

The emphasis in the present studies is on thermochemistry and molecular structure. Paralleling the development of experimental techniques for the study of free radicals, ab initio molecular calculations have improved to the level of "chemical accuracy" for small systems. The synergistic interaction of experiment and theory has greatly enhanced our understanding of both energetics and structure. The example of SiH_4^+ (vide supra) is a case in point.

The free-radical studies summarized in the next section encompass primarily the hydrides of groups III–VI and are organized by group (column) of the periodic chart. Where bond energies or heats of formation are given for neutral species, they are based on a combination of appearance potentials from stable species and adiabatic ionization potentials of free radicals, i.e.,

$$AB + h\nu \rightarrow A^+ + B + e \quad (1)$$

$$A + h\nu \rightarrow A^+ + e \quad (2)$$

from which $D_0(A\text{–}B) = \Delta H_0(1) - \Delta H_0(2)$.

A. The Group V and Group VI Hydrides

1. Molecular Structure. The focus of interest here is the structure of the dihydride ions of group V. The lowest lying states are expected to be $^3B_1$ and $^1A_1$, as in the isoelectronic group IV neutral dihydrides. Quantum chemical calculations at various levels[13] agree that the H–Pn–H angle (Pn = pnicogen) for $^3B_1$ is more obtuse than $^1A_1$ for all Pn investigated. For example,

(12) Dyke, J. M.; Jonathan, N.; Morris, A.; Ridha, A.; Winter, M. J. Chem. *Phys.* **1983**, *81*, 481.

(13) See, for example, ref 8a. For AsH_2^+, calculations have been performed by K. Balasubramanian (*J. Chem. Phys.* **1989**, *91*, 2443) and by L. A. Curtiss (private communication).

Table I
Comparison of Experimental Pn–H_n Bond Energies (Pn = N, P, As) with the Semiempirical Predictions of Goddard and Harding and ab Initio Calculations (in kcal/mol at 0 K)

bond	semi-empirical[a]	Δ	exptl	Δ′	ab initio[e]
$D_0(H_2N\text{–}H)$	101.39		106.7 ± 0.3[b]		105.8
		9.16		15.7	
$D_0(HN\text{–}H)$	92.23		91.0 ± 0.5[b]		91.2
		9.16		12.0	
$D_0(N\text{–}H)$	83.07		79.0 ± 0.4[b]		77.2
$D_0(H_2P\text{–}H)$	81.11		82.5 ± 0.5[c]		81.4
		5.42		7.8	
$D_0(HP\text{–}H)$	75.69		74.7 ± 0.5[c]		75.4
		5.42		4.6	
$D_0(P\text{–}H)$	70.27		70.1 ± 0.5[c]		67.6
$D_0(H_2As\text{–}H)$	74.89		74.9 ± 0.2[d]		
		5.14		8.4	
$D_0(HAs\text{–}H)$	69.75		66.5 ± 0.2[d]		
		5.15		1.9	
$D_0(As\text{–}H)$	64.60		64.6 ± 0.7[d]		

[a] Reference 25. [b] Reference 10. [c] Reference 11 and references therein. [d] Reference 19. [e] Reference 23.

in NH_2^+, this angle is 155° for $^3B_1$ and 100° for $^1A_1$; in PH_2^+, it is 121° 24′ for $^3B_1$ and 93° 24′ for $^1A_1$. To determine the relative *energies* of these states reliably, a fairly sophisticated ab initio calculation is necessary. By application of the Franck–Condon principle, the experimental results (both PES and PIMS) provide a clear answer. In neutral NH_2 (ground state), this angle is 103°.[14] Hence, assuming that the N–H bond distances do not alter significantly (borne out by calculation), the Franck–Condon band for an ionizing transition to $^1A_1$ should be narrow (small change in angle) while the corresponding transition to $^3B_1$ should be broad. In Figure 2a, one sees a broad envelope of vibrational structure near threshold and a single sharp peak at higher energy. We can readily conclude that $^3B_1$ lies lower in energy than $^1A_1$ in NH_2^+, as it does in the isoelectronic CH_2. The same conclusion can be drawn from Figure 2b. Here, the sharp structure corresponds to autoionization of Rydberg states, whose convergence limit is $^1A_1$. These Rydberg states have geometries approaching that of the ionic core ($^1A_1$) and, hence, have sharp Franck–Condon profiles. The $^3B_1$–$^1A_1$ energy difference for NH_2^+ is 30.1 kcal/mol,[10] much larger than for CH_2 (9.04 kcal/mol).[15]

For PH_2^+, the experimental results of Figure 3a,b indicate a reversal. The sharp structure appears at lower energy than the broad structure. Hence, $^1A_1$ lies lower than $^3B_1$, as it does in the isoelectronic SiH_2.[7] The energy difference in SiH_2 is 21.0 ± 0.7 kcal/mol.[7,16–18] As noted earlier, we do not yet know the adiabatic onset of the first excited state in PH_2^+, but an estimate from our data[11] is 16 kcal/mol. We now know that this inversion ($^1A_1$ lower than $^3B_1$) continues[19] for AsH_2^+ and, very likely, GeH_2.[20–22]

(14) Chase, M. W., Jr.; Davies, C. A.; Downey, J. R., Jr.; Frump, D. J.; McDonald, R. A.; Syverud, A. N. JANAF Thermochemical Tables. *J. Phys. Chem. Ref. Data* **1985**, *14*, Suppl. No. 1.

(15) McKellar, A. R. W.; Bunker, P. R.; Sears, T. J.; Evenson, K. M.; Saykally, R. J.; Langhoff, S. R. *J. Chem. Phys.* **1983**, *79*, 5251.

(16) Curtiss, L. A.; Pople, J. A. *Chem. Phys. Lett.* **1988**, *88*, 1775.

(17) Bauschlicher, C. W., Jr.; Langhoff, S. R.; Taylor, P. R. *J. Chem. Phys.* **1987**, *87*, 387.

(18) Balasubramanian, K.; McLean, A. D. *J. Chem. Phys.* **1986**, *85*, 5117.

(19) Berkowitz, J. *J. Chem. Phys.* **1988**, *89*, 7065.

2. Thermochemistry and Bond Energies. We have measured the successive bond energies in the group V and group VI hydrides by the application of the principles contained in eq 1 and 2. These experimental results are listed in Table I for group V hydrides and compared with ab initio calculations.[23] The results for group VI hydrides are published elsewhere.[24] Also shown in this table are semiempirical calculations by Goddard and Harding,[25] which assume purely covalent bonding and use two parameters (the total atomization energy and the p–p′ exchange integral), both obtainable from experiment. The agreement between the experimental results and ab initio calculations is, in almost every case, within the anticipated calculational error of ±2 kcal/mol. The comparison with the semiempirical calculations is also quite satisfactory, providing support not only for the qualitative feature that the bond energy increases with each successive addition of H atoms but also for the quantitative increment, which is predicted to be $\Delta = {}^1/_2$ the p–p′ exchange integral. This is a marked improvement over Pauling's average single bond energy.[26] Deviations from this behavior, particularly for the first-row elements where the assumption of pure covalency is most suspect, are discussed in detail elsewhere.[19]

B. The Group IV Hydrides

We limit ourselves here to recent studies on C_2H_3, C_2H_5, and SiH_n (n = 1–3).

1. Molecular Structure. (a) C_2H_3 and C_2H_5. It is convenient to discuss the vinyl and ethyl radicals together, since there are many similarities in their photoionization behavior. The geometrical structure of C_2H_3 is close to that of ethylene, with a hydrogen atom removed;[27] analogously, the structure of C_2H_5 in its ground state resembles that of ethane.[28] The structure of the corresponding cations in their ground states has not been established by spectroscopic methods. Ab initio calculations predict that a nonclassical, hydrogen-bridged structure lies 1–4 kcal/mol lower[29] than a classical (C_{2v}) structure for $C_2H_3^+$ and about 6 kcal/mol lower[30] than a classical structure for $C_2H_5^+$. Photoionization studies can be related to these possible structures by two criteria: (1) the shape of the photoion yield curve near threshold, which should display a very gradual rise if there is a large change in geometry, and (2) the value of the experimental adiabatic ionization potential compared to that obtained by modern, extensive ab initio calculations for the structures involved. The photoion yield curve of $C_2H_3^+$ is shown in Figure 4a,b.[31] The C_2H_3 has been produced by the F + C_2H_4 reaction and also by pyrolysis of divinylmercury. The approach to the adiabatic onset is very gradual. An upper limit of 8.59 ± 0.03 eV ≡ 1443 ± 5 Å can be deduced. The calculated[29b] adiabatic ionization potential is 8.42 ± 0.1 eV. Both criteria described above favor the nonclassical, bridged structure for $C_2H_3^+$. Similar behavior is observed in the photoionization of ethyl radical,[32] where the adiabatic ionization potential

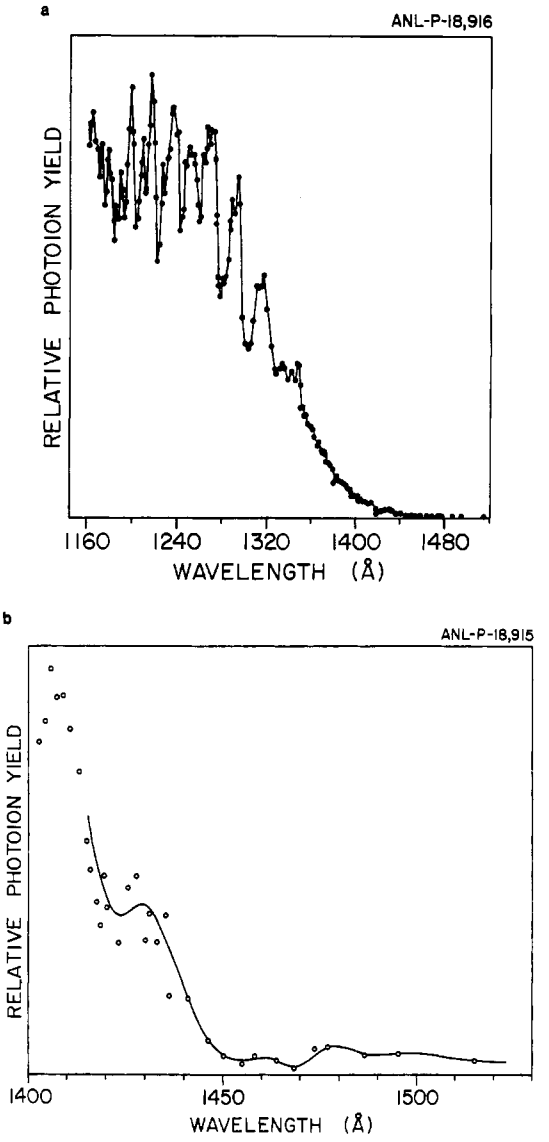

Figure 4. (a) The photoion yield curve of C_2H_3, produced by the F + C_2H_4 reaction. The shorter wavelength region reveals autoionizing structure of vibronic Rydberg states converging to a triplet excited state of $C_2H_3^+$. Reprinted with permission from ref 31. Copyright 1988 American Institute of Physics. (b) An expanded view of the threshold region of part a. The smooth curve is a spline fit to the experimental points. The onset is weak and gradual, characteristic of a large change of geometry in the transition.

(20) Phillips, R. A.; Buenker, R. J.; Beardsworth, R.; Bunker, P. R.; Jensen, P.; Kraemer, W. P. *Chem. Phys. Lett.* **1985**, *118*, 60.
(21) Pettersson, L. G. M.; Siegbahn, P. E. M. *Chem. Phys.* **1986**, *105*, 355.
(22) Balasubramanian, K. *J. Chem. Phys.* **1988**, *89*, 5731.
(23) Pople, J. A.; Luke, B. T.; Frisch, M. J.; Binkley, J. S. *J. Phys. Chem.* **1985**, *89*, 2198. Pople, J. A.; Head-Gordon, M.; Fox, D. J.; Raghavachari, K.; Curtiss, L. A. *J. Chem. Phys.* **1989**, *90*, 5622. For SeH: Balasubramanian, K.; Liao, M. Z.; Han, M. *Chem. Phys. Lett.* **1987**, *139*, 551.
(24) Berkowitz, J. *Radiat. Phys. Chem.* **1988**, *32*, 23.
(25) Goddard, W. A., III; Harding, L. B. *Annu. Rev. Phys. Chem.* **1978**, *29*, 363.
(26) Pauling, L. *The Nature of the Chemical Bond*, 3rd ed.; Cornell University Press: Ithaca, 1960.
(27) Hunziker, H. E.; Kneppe, H.; McLean, A. D.; Siegbahn, P.; Wendt, H. R. *Can. J. Chem.* **1983**, *61*, 993.
(28) (a) Pacansky, J.; Dupuis, M. *J. Chem. Phys.* **1978**, *68*, 4276. (b) Pacansky, J.; Schrader, B. *J. Chem. Phys.* **1983**, *78*, 1033.
(29) (a) Lindh, R.; Roos, B. O.; Kraemer, W. P. *Chem. Phys. Lett.* **1987**, *139*, 407. (b) Curtiss, L. A.; Pople, J. A. *J. Chem. Phys.* **1988**, *88*, 7405. (c) Lee, T. J.; Schaefer, H. F., III *J. Chem. Phys.* **1986**, *85*, 3437. (d) Pople, J. A. *Chem. Phys. Lett.* **1987**, *137*, 10.
(30) (a) Raghavachari, K.; Whiteside, R. A.; Pople, J. A.; Schlayer, P. v. R. *J. Am. Chem. Soc.* **1981**, *103*, 5649. (b) Zurawski, B.; Ahlrichs, R.; Kutzelnigg, W. *Chem. Phys. Lett.* **1973**, *14*, 385. (c) Lischka, H.; Kohler, H.-J. *J. Am. Chem. Soc.* **1978**, *100*, 5297.
(31) Berkowitz, J.; Mayhew, C. A.; Ruscic, B. *J. Chem. Phys.* **1988**, *88*, 7396.
(32) Ruscic, B.; Berkowitz, J.; Curtiss, L. A.; Pople, J. A. *J. Chem. Phys.* **1989**, *91*, 114.

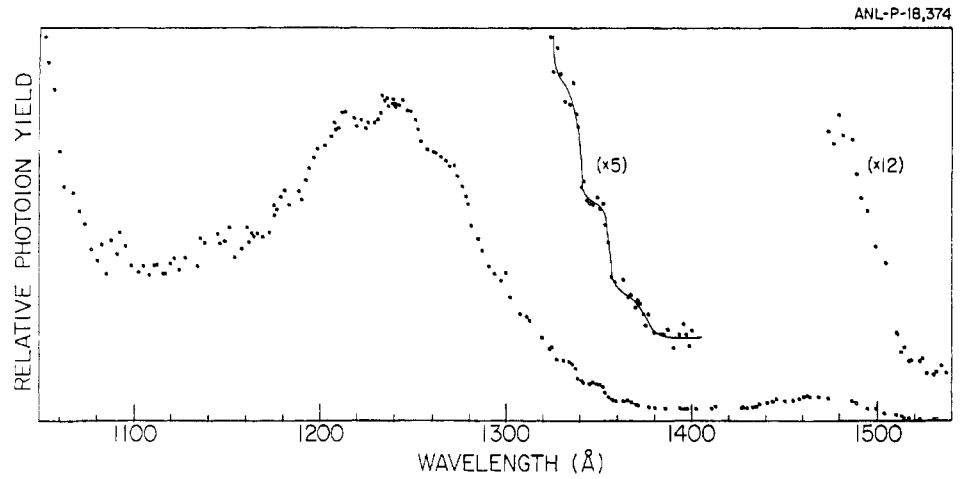

Figure 5. The photoion yield curve of SiH_2, produced by the successive abstraction of H atoms from SiH_4 by F atoms. The data display two onsets, indicative of photoionization from both $\tilde{X}^1A_1$ and $^3B_1$ states of SiH_2. Reprinted with permission from ref 7. Copyright 1987 American Institute of Physics.

is observed experimentally to be 8.117 ± 0.008 eV and is calculated to be 8.06 ± 0.1 eV. In fact, the current calculations for both $C_2H_3^+$ and $C_2H_5^+$ predict that the classical structure for the ground state is not a local minimum, but rather a saddle point on the respective potential surfaces. The PES of ethyl radical[33] reveals vibrational fine structure culminating in an adiabatic IP of 8.26 ± 0.02 eV, close to the presumed onset of the classical structure, but distinctly above that of the nonclassical structure.

In Figure 4a, rather prominent structure can be observed at the shorter wavelengths. This is attributed to autoionization of vibronic components of Rydberg states converging to a higher ionization potential. The higher IP corresponds to a triplet state, with a "classical" structure similar to that of neutral C_2H_3, but with a longer C–C bond. A similar situation exists in C_2H_5, although the structure is not as prominent. Thus, we conclude that the ground state singlet structures of $C_2H_3^+$ and $C_2H_5^+$ are bridged, while the first excited (triplet) states are classical.

(b) The SiH_n Species. We have already noted how ionization distorts the tetrahedral SiH_4 to a $SiH_2^+ \cdot H_2$ entity. For SiH_3, both PES[12] and PIMS[7] have revealed a vibrational progression, interpretable as a transition from pyramidal $SiH_3(\tilde{X}^2A_1)$ to planar SiH_3^+. The surprising result of the PIMS study was the observation that SiH_2 and SiH were also generated in sufficient abundance for experimental study, the former in both its metastable $^3B_1$ and ground $^1A_1$ states. Figure 5 displays this spectrum, from which it was possible to extract both ionization potentials, and hence the only significant experimental value to date of this $^3B_1$–$^1A_1$ splitting.

2. Thermochemistry and Bond Energies. (a) C_2H_3–H and C_2H_5–H. At the time of our experimental study,[31] the C–H bond energy in ethylene was uncertain, values ranging from 100 to 117 kcal/mol. Our value, based on the aforementioned IP of C_2H_3 and the appearance potential of $C_2H_3^+$ from C_2H_4, is 107–110 kcal/mol. Ab initio calculations[29b] and other recent experiments[34] corroborate this value. By contrast, the C–H bond energy in ethane was found to be 99.6 ± 0.6 kcal/mol, consistent with earlier values. The C–H bond energy in acetylene is currently in dispute. Some favor $132._6 \pm 1._2$ kcal/mol.[35] A very recent study[36] concludes that the upper limit is 126.65 kcal/mol.

Table II
Recently Reported Bond Energies (kcal/mol) in the SiH_n Series (0 K)

	Pople et al.[a]	Ho et al.[b]	Walsh[c]	PIMS[d]
Si–H	69.8	67.4	69.2	68.7 ± 0.7
HSi–H	76.2	74.1	82.3	75.6 ± 1.4
H_2Si–H	66.8	71.0	61.5	≥67.3
H_3Si–H	91.7	90.1	88.3	≤91.1
total	304.5	302.6	301.3	302.7

[a] Reference 23. For a slightly corrected value, see also: Curtiss, L. A.; Pople, J. A. *Chem. Phys. Lett.* **1988**, *144*, 38. [b] Ho, P.; Coltrin, M. E.; Binkley, J. S.; Melius, C. F. *J. Phys. Chem.* **1985**, *89*, 4647. [c] Reference 37. [d] Reference 7. Here, $D_0(H_3Si–H)$ is based on $AP(SiH_3^+) \leq 12.086$ eV from ref 7 and the recently determined $IP(SiH_3) = 8.135^{+5}_{-2}$ eV from Johnson et al. (Johnson, R. D., III; Tsai, B. P.; Hudgens, J. W. (preprint)) rather than that of ref 37.

(b) SiH_n Species. The heats of formation of the various SiH_n species were thought to be well-established at the time of an Account by Walsh.[37] His equivalent stepwise bond energies are shown in column 2 of Table II. Subsequently, some evidence suggested that $\Delta H_f(SiH_2)$ was in error. Columns 3 and 4 are results of recent ab initio calculations of these bond energies. Column 5 represents our experimental results, based on studies of the SiH, SiH_2, and SiH_3 ionization potentials. Our experimental results indicate that Walsh's value of $\Delta H_f°(SiH_2)$ was in error and are in fairly good agreement with the ab initio calculations.

C. The Group III Hydrides

Our activities in this area have thus far been limited to the simple boron hydrides. Two types of free-radical experiments have been performed, one in which BH_3 was generated by pyrolysis of B_2H_6, the other a reaction of F with B_2H_6, producing B_2H_5 and B_2H_4.

1. Molecular Structure. The structure of the simplest stable borohydride species, B_2H_6, has been established for about 40 years as a dibridged, D_{2h}

(33) Dyke, J. M.; Ellis, A. R.; Keddar, N.; Morris, A. *J. Phys. Chem.* **1984**, *88*, 2565.
(34) Cited in ref 29.
(35) (a) Wodtke, A. M.; Lee, Y. T. *J. Phys. Chem.* **1985**, *89*, 4744. (b) Curtiss, L. A.; Pople, J. A. *J. Chem. Phys.* **1989**, *91*, 2420.
(36) Green, P. G.; Kinsey, J. L.; Field, R. W. A New Determination of the Dissociation Energy of Acetylene. *J. Chem. Phys.* Submitted.
(37) Walsh, R. *Acc. Chem. Res.* **1981**, *14*, 246.

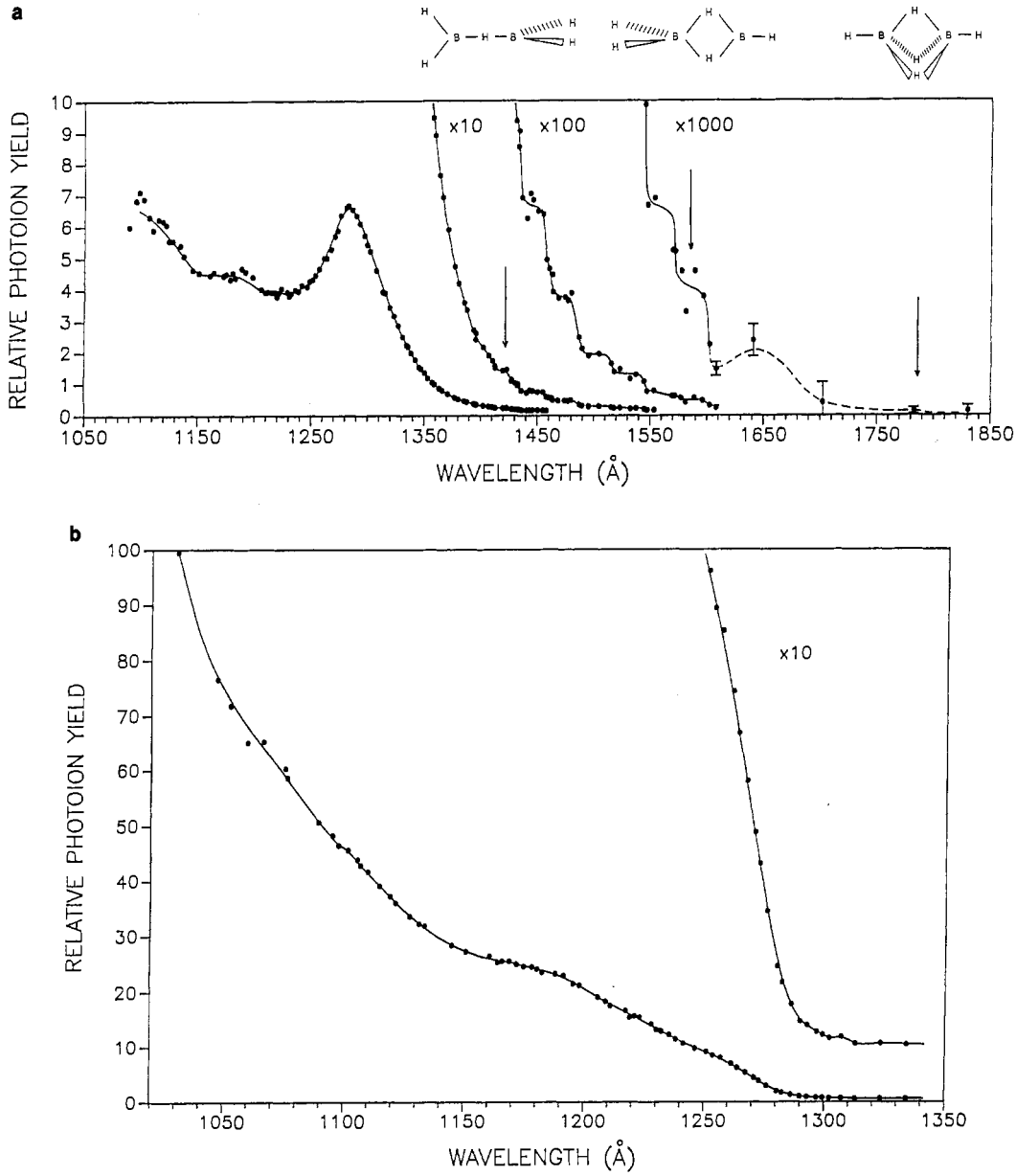

Figure 6. (a) Photoion yield curve of $B_2H_5^+$ (B_2H_5), where B_2H_5 is produced by the F + B_2H_6 reaction. Arrows indicate the adiabatic thresholds obtained by ab initio calculations (ref 39) for the ionic structures shown. Reprinted with permission from ref 41. Copyright 1989 American Institute of Physics. (b) Photoion yield curve of $B_2H_3^+$ (B_2H_5). The ordinate scales of parts a and b are matched, i.e., $B_2H_3^+$ and $B_2H_5^+$ from B_2H_5 are equal in intensity at ca. 1265 Å.

structure. Upon photoionization,[38] a very weak $B_2H_6^+$ ion is formed, and almost at the ionization threshold, a very strong $B_2H_5^+$ signal is observed. This behavior has been rationalized by recent ab initio calculations,[39] which predict that the most stable $B_2H_5^+$ structure is *tribridged* (D_{3h}), and $B_2H_6^+$ is best described as a very weak $B_2H_5^+ \cdot H$. On the ground state potential surface of $B_2H_5^+$, there also exist a local minimum 20.2 kcal/mol higher in energy, corresponding to a dibridged (C_{2v}) structure, and a saddle point 41.0 kcal/mol higher, corresponding to a singly bridged (D_{2d}) structure. By contrast, very recent calculations[40] for neutral B_2H_5 indicate that the most stable structure is singly bridged, about 3–5 kcal/mol lower in energy than a dibridged structure.

We have just examined the photoionization of B_2H_5[41] and observed very unusual behavior. The photoion yield curve is vanishingly small near threshold (~6.95 eV) and then very gradually increases to a maximum $B_2H_5^+$ production at least 3 orders of magnitude larger at 9.67 eV ≡ 1282 Å (Figure 6a). At about this energy, the fragment $B_2H_3^+$ first appears, and it ultimately exceeds $B_2H_5^+$ by another order of magnitude (see Figure 6b). This behavior would have been very surprising in the absence of ab initio calculations, but a posteriori, it provides strong verification for both calculations. An ionizing transition from a singly bridged B_2H_5 to a tribridged $B_2H_5^+$ can be expected to have vanishingly small Franck–Condon factors. The transition probability is not expected to be enhanced greatly at the energy onset of the dibridged cationic structure, but can be expected to reach a maximum in the vicinity

(38) Ruscic, B.; Mayhew, C. A.; Berkowitz, J. *J. Chem. Phys.* **1988**, *88*, 5580.
(39) Curtiss, L. A.; Pople, J. A. *J. Chem. Phys.* **1988**, *89*, 4875.
(40) Trachtman, M.; Bock, C. W.; Niki, H.; Mains, G. J. *J. Struct. Chem.* In press.
(41) Ruscic, B.; Schwarz, M.; Berkowitz, J. *J. Chem. Phys.* **1989**, *91*, 4183.

of the saddle point representing the singly bridged ionic form.

The steplike structure at intermediate energies is currently believed to be due to ionization of the isomeric, dibridged neutral species to the dibridged ionic form, the steps corresponding to a vibrational progression involving a distortion of the B–H–B–H bridge. There is also evidence in our data for an excited state of $B_2H_5^+$, which has sufficient intensity to suggest a singly bridged structure, and which branches into both $B_2H_5^+$ parent and $B_2H_3^+$ fragment ions.

Ab initio calculations[42,43] on B_2H_4 predict stability for this species, but it has eluded experimental identification prior to our studies. The most recent calculations[44] verify that a B–B-bonded D_{2d} structure and a dibridged C_{2v} structure, almost exactly degenerate, represent the neutral ground state, and indicate that the most stable cationic state is dibridged C_{2v}, with a tribridged structure lying 11.4 kcal/mol higher, and a B–B-bonded D_{2d} structure 19.0 kcal/mol higher. Our photoion yield curve is steplike, but rises rather abruptly, in marked contrast to the photoionization behavior of B_2H_5. The shape of the photoion yield curve and the experimentally obtained adiabatic ionization potential are consistent with the calculated C_{2v} structures for both neutral B_2H_4 and ground-state $B_2H_4^+$. This result does not preclude the possible coexistence of the D_{2d} structure of B_2H_4, since its transition probability to the C_{2v} structure of $B_2H_4^+$ can be expected to be small in the threshold region. In fact, a $B_2H_2^+$ fragment is observed at higher energy, which may well result from the sequential process $B_2H_4(D_{2d}) + h\nu \rightarrow B_2H_4^+(D_{2d}) \rightarrow B_2H_2^+ + H_2$.

Calculations[45] indicate that BH_3 is planar (D_{3h}), but that the lowest ionization energy corresponds to a degenerate state, subject to Jahn–Teller distortion. Our experimental photoion yield curve[38] is consistent with this interpretation.

2. Thermochemistry and Bond Energies. We have shown[38] that the direct application of eq 1 and 2 to determine the dimerization energy of BH_3 by measuring its ionization potential and its appearance potential from B_2H_6 is inappropriate for this system. However, a rather lengthy analysis[38] of the data leads to a dimerization energy of 34.3–39.1 kcal/mol, in good agreement with ab initio calculations.[39,46] Preliminary results from our B_2H_5 and B_2H_4 studies indicate that $D_0(B_2H_5\text{–H}) \lesssim 102.7$ kcal/mol, but $D_0(B_2H_4\text{–H})$ is much weaker, ~40.1 kcal/mol.

Prospects for Future Work

There are many other free radicals (besides the compact, but confining category of hydrides described in this Account) that are of both fundamental and practical importance that should be amenable to study by the PIMS method. One example is COOH, an important combustion intermediate, which we have recently studied[47] for the first time in the gas phase. The utilization of some form of photoion–photoelectron coincidence technique will ultimately provide detailed PES information, without the superposition problem. More intense light sources, such as the advanced light source currently under construction, should provide greater sensitivity and improved signal-to-noise. It may then be possible to utilize known spectral features in order to examine the role of these radicals as intermediates in specific chemical reactions. Certain radicals that are difficult to prepare because of rapid wall reactions or reactions with precursors could be prepared by laser photodissociation in a crossed-beam apparatus. Direct structural studies of radicals and cations by laser techniques will provide more detailed information than is currently available from Franck–Condon analysis and ab initio calculations. With such advances, less intrusive diagnostic techniques such as laser-induced fluorescence could monitor the formation and reaction of these intermediates in chemical reactions.

The experimental work performed in the author's laboratory and cited in this Account was carried out in collaboration with several colleagues, including Drs. B. Ruscic, S. T. Gibson, H. Cho, C. A. Mayhew, and M. Schwarz. The work was supported by the U. S. Department of Energy, Office of Basic Energy Sciences, Division of Chemical Sciences, under Contract W-31-109-Eng-38.

Registry No. C_2H_5, 2025-56-1; C_2H_3, 2669-89-8; SiH, 13774-94-2; SiH_2, 13825-90-6; SiH_3, 13765-44-1; BH_3, 13283-31-3; B_2H_5, 52227-38-0; B_2H_4, 18099-45-1.

(42) Vincent, M. A.; Schaefer, H. F., III *J. Am. Chem. Soc.* **1981**, *103*, 5679.
(43) Mohr, R. A.; Lipscomb, W. N. *Inorg. Chem.* **1986**, *25*, 1053.
(44) Curtiss, L. A.; Pople, J. A. *J. Chem. Phys.* In press.
(45) Curtiss, L. A.; Pople, J. A. *J. Phys. Chem.* **1988**, *92*, 894.
(46) Page, M.; Adams, G. F.; Binkley, J. S.; Melius, C. F. *J. Phys. Chem.* **1987**, *91*, 2675.
(47) Ruscic, B.; Schwarz, M.; Berkowitz, J. *J. Chem. Phys.* In press.